10.24425/acs.2025.157143

*Archives of Control Sciences*
*Volume* 35(LXXI), 2025
*No.* 4, *pages* 683–712

# Integrated planning and control method for autonomous driving considering user's steering style

Meng WANG, Juexuan CHEN, Xue LV, Shiyun ZHU and Shengping DAI

In response to the lack of adaptability to individual differences in driving style for autonomous vehicles, an integrated planning and control method for autonomous driving that considers user's steering style is proposed. Based on the artificial potential field theory, a vehicle motion path evaluation model is constructed, and the optimization goal is set as a comprehensive performance index of safety, comfort, and accuracy. The mathematical model of the integrated planning and control system for autonomous driving is established. Using natural driving data from user, a least squares method is employed to generate personalized steering style curves. A decoding method based on steering style factors is proposed, followed using genetic algorithms to solve the optimization problem of integrated planning and control, obtaining the optimal steering control quantity that conforms to the user's driving style and implementing personalized vehicle automatic steering control. Simulation experiments have verified the feasibility of the integrated planning and control strategy considering user's steering style in typical driving scenarios, completing the identification and adaptation of user personalized steering style, and achieving the resolution of conflicts between autonomous driving and user's driving style.

**Key words:** autonomous driving, driving style, integrated planning and control, steering style curve, genetic algorithm

## 1. Introduction

The significance of personalized autonomous driving technology lies in enhancing user trust and improving user experience. Current research on personalized autonomous driving mainly focuses on the decision-making level, where



M. Wang (e-mail: wangmwuhan@aliyun.com), X. Lv (corresponding author, e-mail: lvxueer200@163.com) and S. Dai (e-mail: 3787366652@qq.com) are with School of Mechanical and Electrical Engineering, Changjiang Institute of Technology, Wuhan, China.

J. Chen (e-mail: juexuanchen@hotmail.com) and S. Zhu (e-mail: shiyunz@goyu-ai.com) are with the Department of Autonomous Driving, Wuhan Goyu Intelligent Technology Co., Ltd., Wuhan, China.

The authors were supported by the Hubei Provincial Natural Science Foundation of China (2024AFB897).

Received 08.12.2024.

machine learning methods are used to mimic human habits for driving decisions. For instance, relevant studies have analyzed the personalized characteristics of drivers and defined driving styles as conservative, moderate, and aggressive types [1, 2], designing driving decision parameters accordingly to enable autonomous vehicles to make driving decisions according to these three specific styles.

The path planning and steering control of intelligent vehicles determine the amplitude of the vehicle's steering actions, which directly affects the user's riding experience. When the driving path and longitudinal and lateral control styles of an intelligent car are consistent with the user's personalized driving style, the user's trust will significantly increase [3,4], enhancing consumers' acceptance of intelligent cars [5,6]. Therefore, considering the user's driving style and designing path planning and steering control strategies accordingly to resolve conflicts between autonomous driving planning and control and personalized driving is of great research significance.

Traditional autonomous driving planning and control strategies are mostly based on the "plan-then-follow control" concept, where the planning layer first finds a collision-free path, and then the following controller calculates the steering wheel angle to control the vehicle along the planned path [7]. The traditional layered planning and control method can decouple the problem modules, reducing the complexity of problem solving, which is why the layered method currently receives more attention [8]. The consequence of separating planning and control is that the path obtained by the planning layer violates the vehicle's kinematic characteristics, and this problem spreads to the following control layer, ultimately leading to poor vehicle driving behavior quality [9, 10]. On the other hand, the parameter tuning of the layered planning control strategy is relatively fixed, lacking an adaptation mechanism for users' driving styles, requiring adaptive adjustment of driving style parameters to resolve human-machine driving style conflicts [11]. Data-driven end-to-end planning control strategies are limited by large-scale training of annotated data, leaning towards generalized driving styles [12], and cannot meet user personalized driving needs. Relevant research introduces aggressive, moderate, and conservative driving styles into planning and control, allowing users to choose among three planning control styles. This discrete driving style approach can alleviate driving style conflicts but still falls short of accommodating the more subtle differences between different drivers [13].

Traditional planning and control methods cannot adapt to users' personalized driving habits, often leading to dissatisfaction among aggressive driving style users with conservative steering strategies of intelligent vehicles, or concerns among conservative driving style users with aggressive steering strategies of intelligent vehicles. In response to the issues, this paper studies an integrated

strategy for autonomous driving planning and control that considers user's steering style. By collecting and analyzing natural driving data from user, the steering style curves of user are identified, and steering style factors are integrated into the integrated planning and control. Genetic algorithms are used to solve the optimization problem of integrated planning and control, enabling intelligent vehicles to implement steering control according to the user's personalized style. The innovations of this paper are: (1) An integrated planning and control optimization model is constructed based on artificial potential field theory, addressing the issue of poor control quality in traditional planning and control strategies; (2) Personalized user's steering style is identified based on natural driving data, and steering control quantities that conform to user's driving style are solved accordingly, achieving the anthropomorphic driving goal at the planning and control layer. The structure of the rest of this paper is as follows: First, in Section 2, a vehicle motion path evaluation model is constructed based on artificial potential field theory to evaluate and model the planned path. In Section 3, an integrated planning and control optimization problem mathematical model is constructed based on optimal control theory. Then, in Section 4, driving style curves are generated by fitting using the least squares method based on the obtained user's natural driving data. In Section 5, a genetic algorithm based on steering style factors is proposed, and the optimal steering control quantity for the integrated planning and control problem is solved through iterative evolution, implementing intelligent vehicle steering control. In Section 6, simulation experiments in typical scenarios are designed to verify the feasibility of the integrated planning and control strategy considering user's steering style. Finally, Section 7 summarizes and prospects the study.

## 2. Evaluation model of motion path

The traditional artificial potential field method introduces the concept of a virtual potential field for planning the driving path of intelligent vehicles [14]. This section is based on the artificial potential field theory to evaluate and model the vehicle's motion path, designing the lane potential field function, boundary potential field function, obstacle potential field function, and target point potential field function. A motion path evaluation model based on safety performance indicators is constructed to evaluate the safety performance of the vehicle's motion path.

### 2.1. Lane potential field model

Structured roads typically consist of multiple lanes, with a high safety index when intelligent vehicles drive in the center of the lane and a low safety index when driving near the lane boundaries. By designing a lane potential field function, the safety performance of the intelligent vehicle's driving path is described. Assuming

that the vehicle's motion path point is in the $i$-th lane, the lane potential field function value of this path point is defined as:

$$U_{\text{lane}} = A_{\text{lane}} \exp\left(-\frac{(y - y_{\text{lane},i})^2}{2\sigma_{\text{lane}}^2}\right). \tag{1}$$

In the formula: $y_{\text{lane},i}$ is the distance from the vehicle's driving path point to the centerline of the $i$-th lane; $A_{\text{lane}}$ is the lane potential field coefficient; and $\sigma_{\text{lane}}$ is the lane width parameter.

Figure 1a shows the lane potential field diagram of a structured road, where the $X$-axis is the road forward distance, the $Y$-axis is the road lateral distance, and the $Z$-axis is the normalized potential field strength. The potential field strength is lowest at the center of each lane and highest at the positions of the lane boundaries. Under the action of steering control quantities, the smaller the lane potential field function value of the vehicle's motion path, the better the steering control quantity.

### 2.2. Boundary potential field model

The left and right boundaries of structured roads are crucial for the safety of intelligent vehicle driving. It is generally required that the motion path of intelligent vehicles should be within the left and right boundaries of the road and as far away from the road boundaries as possible to avoid accidents caused by exceeding the boundaries. Assuming the left and right boundary lines are $i = 1$ and $i = 2$ respectively, the road boundary potential field function is defined as:

$$U_{\text{border},i} = A_{\text{border}} \left(\frac{1}{y - y_{\text{border},i}}\right)^2. \tag{2}$$

In the formula: $y - y_{\text{border},i}$ is the distance from the path point to the left or right boundary line, taking the closer boundary line distance; $A_{\text{border}}$ is the boundary potential field coefficient. At the same time, when the path point exceeds the boundary line range, the boundary potential field value is defined as $+\infty$.

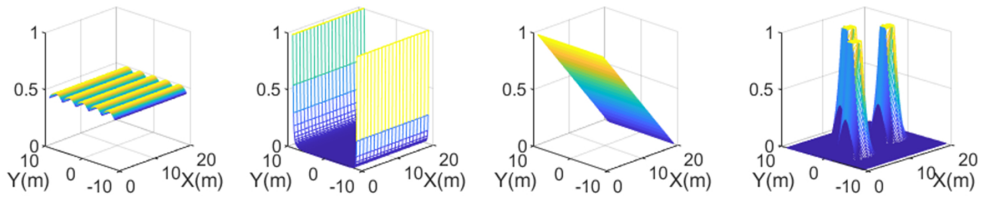


(a) (b) (c) (d)

Figure 1: Potential field model: (a) lane potential field; (b) boundary potential field; (c) obstacle potential field; (d) target point potential field

Figure 1b shows the boundary potential field diagram. $Y = 0$ is the road centerline, and the potential field strength is lowest at the position of the road centerline and $+\infty$ at the positions of the lane boundaries. Under the action of steering control quantities, the smaller the boundary potential field function value of the vehicle's motion path, the better the steering control quantity.

### 2.3. Target point potential field function

The target point potential field is used to represent the vehicle's forward driving performance. A virtual target point is set in front of the road, and the closer the vehicle's driving path point is to the target point, the smaller the target point potential field function value. The target point potential field function is defined as:

$$U_{\text{goal}} = A_{\text{goal}}(x - x_{\text{vel}}). \tag{3}$$

In the formula: $x - x_{\text{vel}}$ represents the longitudinal distance from the path point to the virtual target point, and $A_{\text{goal}}$ is the target point potential field coefficient.

Figure 1c shows the target point potential field diagram, where the $X$-axis is the road forward distance. Assuming the virtual target point position is $X = 20$, the potential field strength at the target point position is 0, and the farther the path point is from the virtual target point, the greater the target point potential field strength. Under the action of steering control quantities, the smaller the target point potential field function value of the vehicle's motion path, the better the steering control quantity.

### 2.4. Obstacle Potential Field Model

The obstacle potential field is used to represent the obstacle avoidance performance of the vehicle's driving path. The closer the vehicle's driving path is to the obstacle area, the greater the potential field function value. Based on this principle, the obstacle potential field function is defined as:

$$U_{\text{obs}} = \begin{cases} \dfrac{1}{2}K_b\left(\dfrac{1}{d(\boldsymbol{X}_R, \boldsymbol{X}_O)} - \dfrac{1}{d_0}\right)^2, & d(\boldsymbol{X}_R, \boldsymbol{X}_O) \leqslant d_0\,. \\ 0, & d(\boldsymbol{X}_R, \boldsymbol{X}_O) > d_0\,. \end{cases} \tag{4}$$

In the formula: $\boldsymbol{X}_O = (x_O, y_O)$ is the position of the obstacle (the obstacle is treated as a point mass); $\boldsymbol{X}_R = (x_R, y_R)$ is the position of the vehicle; $d(\boldsymbol{X}_R, \boldsymbol{X}_O)$ is the distance from the path point to the obstacle; and $d_0$ is the influence range of the obstacle potential field, that is, the potential field strength influence is 0 outside the obstacle range $d_0$.

Figure 1d shows the obstacle potential field diagram. Assuming the positions of the obstacles are $(5, -5)$, $(10, 5)$, and $(15, -5)$, then the potential field strength is the greatest at the positions of the obstacles, and the potential field strength is 0 in the areas outside the influence range of the obstacles. Under the action of steering control quantities, the smaller the obstacle potential field function value of the vehicle's motion path, the better the steering control quantity.

### 2.5. Evaluation model of vehicle motion path

The vehicle's motion path points are simultaneously affected by the lane potential field, boundary potential field, obstacle potential field, and target point potential field. Therefore, the global comprehensive potential field function is constructed as the sum of the potential fields:

$$U_{\text{field}} = U_{\text{lane}} + U_{\text{road}} + U_{\text{obs}} + U_{\text{goal}} \,. \tag{5}$$

As shown in Figure 2, which is the global potential field diagram of the road, the smaller the comprehensive potential field function value of the vehicle's motion path under the action of steering control quantities, the better the steering control quantity. The vehicle's motion path should extend forward in the direction of the weakest global comprehensive potential field, that is, the potential field function value of the optimal driving path in the global potential field is the smallest.

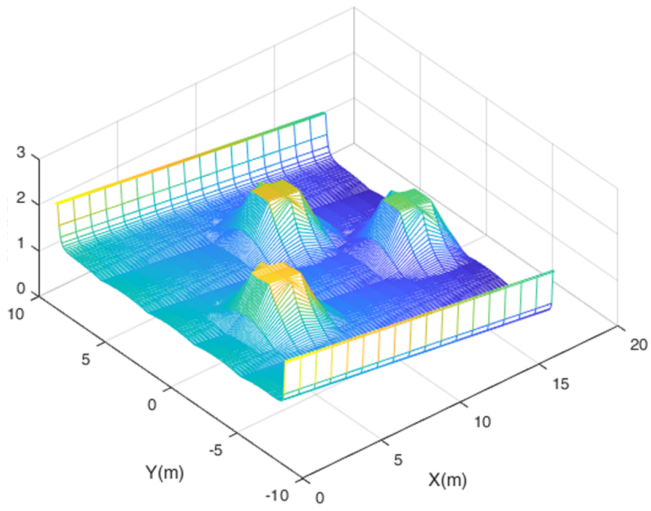


Figure 2: Global potential field

The motion path of the intelligent vehicle is represented as a set of path points $\boldsymbol{\Psi} = \{(x_1, y_1),\ (x_2, y_2),\ \ldots,\ (x_N, y_N)\}$, and it is placed in the global potential

field. Then, the comprehensive potential field strength of each path point is $U_{\text{field}}(1)$, $U_{\text{field}}(2)$, ..., $U_{\text{field}}(N)$. The vehicle motion path safety performance evaluation function is defined as the average value of the comprehensive potential field strength of all path points, that is:

$$J_1 = U_{\text{field}}(\boldsymbol{\Psi}) = \frac{1}{N}\sum_{i=1}^{N} U_{\text{field}}(i). \tag{6}$$

## 3. Integrated planning and control mathematical model

The autonomous driving planning and control problem can be stated as: under certain constraint conditions, to find the optimal steering control quantity so that the comprehensive performance of the intelligent vehicle's driving path and execution effect is optimal. This section builds a virtual driving path prediction model for intelligent vehicle based on vehicle motion characteristics and mathematically models the integrated planning and control optimization problem of autonomous driving from three aspects: decision variables, objective function, and constraint conditions.

### 3.1. Integrated planning and control architecture

The autonomous driving planning and control layer takes the environmental recognition information from the perception and positioning layer (including lane information and obstacle information) and the reference path as inputs, and outputs control commands (including front wheel steering angle) to maneuver the vehicle in a comfortable and safe manner. The typical layered planning and control framework is shown in Figure 3a, where the planning layer first plans the target path based on the input information, represented explicitly as a two-dimensional spatial path, and then the control layer calculates and outputs the target front wheel steering angle based on the target path, making the vehicle follow the target path. The layered planning and control strategy, due to its relatively fixed parameter tuning, lacks an adaptation mechanism for user driving styles, and the decoupling of problems leads to poor vehicle driving behavior quality. The data-driven end-to-end planning and control framework is shown in Figure 3b, where the planning and control problem is neural networked, using one or more neural network models to represent the mapping relationship from environmental information input to steering control output, no longer relying on subjective rules preset by engineers [15]. The end-to-end planning and control strategy is limited by large-scale training of annotated data, leaning towards generalized driving styles, and cannot meet user's personalized driving needs.

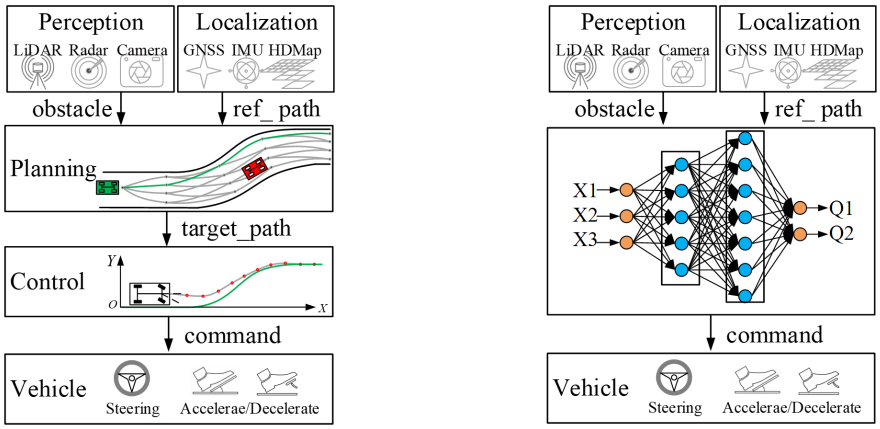


(a) (b)

Figure 3: Planning and control architecture of autonomous driving: (a) layered architecture; (b) End-to-End architecture

To address the issue that traditional planning and control architectures cannot handle conflicts between autonomous driving and user driving styles, this paper constructs an integrated planning and control framework structure. By treating the planning and control layers, an integrated planning and control evaluation function is designed with safety, accuracy, and comfort as the goals, and an integrated planning and control optimization problem mathematical model is constructed. By considering the genetic algorithm optimization solution for user steering styles, the optimal steering control quantity is calculated to achieve anthropomorphic global optimal control of intelligent vehicles. The integrated planning and control architecture is shown in Figure 4.

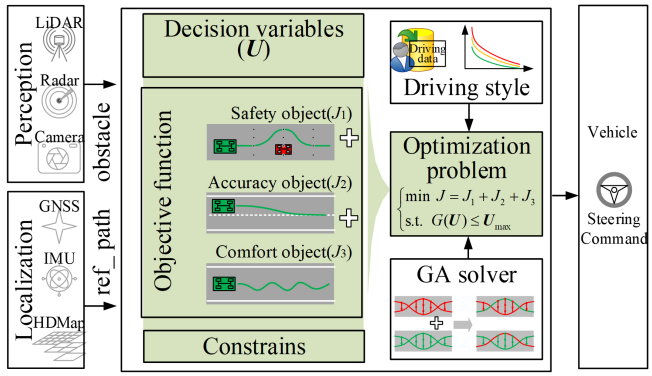


Figure 4: Integrated planning and control architecture of autonomous rriving

### 3.2. Decision variables

The goal of planning and control is to decide on the optimal control quantity, i.e., the decision variable, so that the vehicle can accurately and safely track the reference path according to this decision variable. The decision variable can be a single control quantity or a sequence of control quantities. In optimal control theory, a control sequence over a future time domain is usually designed as the decision variable [16], and the initial decision variable is continuously optimized through iterative optimization strategies. According to the principles of optimal control theory, combined with the characteristics of motion control of autonomous vehicle, the decision variable is designed as a control increment sequence over the future time domain:

$$\Delta \boldsymbol{U} = [\Delta \boldsymbol{u}_0, \Delta \boldsymbol{u}_1, \Delta \boldsymbol{u}_2, \ldots, \Delta \boldsymbol{u}_n, \ldots, \Delta \boldsymbol{u}_{N-1}]^T . \tag{7}$$

In the formula: $\Delta \boldsymbol{u}_n$ is the control increment at time $n$ in the future. For autonomous vehicles, $\Delta \boldsymbol{u}_n = [\delta_n, v_n]^T$, where $\delta_n$ and $v_n$ are the steering control quantity and speed control quantity at time $n$, respectively.

Assuming the output control quantity of the last control cycle is $\boldsymbol{u}_{\text{pre}}$, the control sequence for the next $N$ moments can be inferred based on the decision variable:

$$\boldsymbol{U}(\Delta \boldsymbol{U}) = [\boldsymbol{u}_0, \boldsymbol{u}_1, \boldsymbol{u}_2, \ldots, \boldsymbol{u}_n, \ldots, \boldsymbol{u}_{N-1}]^T . \tag{8}$$

In the formula: $\boldsymbol{u}_n$ is the control quantity at time $n$ in the future, and it satisfies:

$$\boldsymbol{u}_n = \boldsymbol{u}_{\text{pre}} + \Delta \boldsymbol{u}_0 + \Delta \boldsymbol{u}_1 + \Delta \boldsymbol{u}_2 + \cdots + \Delta \boldsymbol{u}_n . \tag{9}$$

Formulas (8), (9) indicate that the control increment sequence, as the decision variable, determines the control sequence for future moments.

### 3.3. Prediction model of motion path

Using the vehicle kinematics model, based on the given initial control variables and future control sequences, the system's future state is predicted through the system's state equations to obtain the virtual driving path of the intelligent vehicle.

Given the system's initial state and control sequence, the dynamic process of the system output can be predicted through the system's state-space equations. For any nonlinear time-varying system, the state equation can be described as:

$$\begin{cases} \dot{\boldsymbol{X}}(t) = f\big(t, \boldsymbol{X}(t), \boldsymbol{u}(t)\big), \\ \boldsymbol{Y}(t) = g\big(t, \boldsymbol{X}(t), \boldsymbol{u}(t)\big). \end{cases} \tag{10}$$

In the formula: $\boldsymbol{X}(t) \in R^n$ is the $n$-dimensional state vector; $\boldsymbol{u}(t) \in R^m$ is the control vector; $f(\cdot)$ is the system's state transition function, $\boldsymbol{Y}(t)$ is the system output, and $g(\cdot)$ is the system's output function.

By discretization processing, the discrete state equation is constructed:

$$\boldsymbol{X}(k+1) = f\big(T, \boldsymbol{X}(k), \boldsymbol{U}(k)\big). \tag{11}$$

In the formula: $\boldsymbol{X}(k)$ and $\boldsymbol{X}(k+1)$ are the state quantities at moments $k$ and $k+1$, respectively, and $T$ is the control cycle.

For autonomous vehicles, the control quantity is $\boldsymbol{u} = [v, \delta]^T$, where $v$ is the target vehicle speed and $\delta$ is the target front wheel steering angle; the state quantity is $\boldsymbol{X} = [x, y, \theta]^T$. $(x, y)$ are the vehicle's planar coordinates, and $\theta$ is the vehicle's heading, with the output quantity $\boldsymbol{Y} = [x, y, \theta]^T = \boldsymbol{I}_{3\times3}\boldsymbol{X}$. Given the initial state quantity $\boldsymbol{X}(0) = [x_0, y_0, \theta_0]^T$ and the control sequence $\boldsymbol{U}(\Delta\boldsymbol{U}) = [\boldsymbol{u}_0\ \boldsymbol{u}_1\ \boldsymbol{u}_2\ \ldots\ \boldsymbol{u}_N]^T$ for the next $N$ moments, the vehicle's future travel state quantity can be predicted based on the state equation:

$$\begin{cases} \boldsymbol{X}(1) = f\big(T, \boldsymbol{X}(0), \boldsymbol{u}_0\big), \\ \boldsymbol{X}(2) = f\big(T, \boldsymbol{X}(1), \boldsymbol{u}_1\big), \\ \boldsymbol{X}(3) = f\big(T, \boldsymbol{X}(2), \boldsymbol{u}_2\big), \\ \qquad \vdots \\ \boldsymbol{X}(N) = f\big(T, \boldsymbol{X}(N-1), \boldsymbol{u}_{N-1}\big), \end{cases} \tag{12}$$

Then, the system output of the vehicle's motion can be expressed as:

$$\boldsymbol{\Psi}(\Delta\boldsymbol{U}) = \begin{bmatrix} \boldsymbol{Y}(1) \\ \boldsymbol{Y}(2) \\ \vdots \\ \boldsymbol{Y}(N) \end{bmatrix} = \begin{bmatrix} \boldsymbol{C}\boldsymbol{X}(1) \\ \boldsymbol{C}\boldsymbol{X}(2) \\ \vdots \\ \boldsymbol{C}\boldsymbol{X}(N) \end{bmatrix} = F\big(T, \boldsymbol{X}(0), \boldsymbol{U}(\Delta\boldsymbol{U})\big). \tag{13}$$

In the formula: $\boldsymbol{C} = \boldsymbol{I}_{3\times3}$.

Taking formula (13) as the vehicle motion path prediction model, based on the prediction model, it is known that given the vehicle's initial state quantity and future control sequence, the vehicle's future motion path $\boldsymbol{\Psi}(\Delta\boldsymbol{U})$ can be determined.

### 3.4. Objective function

The decision variable $\Delta\boldsymbol{U}$ determines the future control sequence $\boldsymbol{U}$ and the vehicle's motion path $\boldsymbol{\Psi}$. Based on the principles of safety, accuracy, and comfort in autonomous driving, an integrated planning and control objective function is designed.

For the intelligent vehicle's motion path $\boldsymbol{\Psi}(\Delta \boldsymbol{U})$, based on the vehicle motion path evaluation model described in Section 1, a safety performance index function is designed as:

$$J_1\big(\boldsymbol{\Psi}(\Delta \boldsymbol{U})\big) = U_{\text{field}}\big(\boldsymbol{\Psi}(\Delta \boldsymbol{U})\big) = \frac{1}{N}\sum_{i=1}^{N} U_{\text{field}}(i). \tag{14}$$

For the intelligent vehicle's motion path $\boldsymbol{\Psi}(\Delta \boldsymbol{U})$, based on the principle of accuracy, it is desired that the motion path $\boldsymbol{\Psi}$ is consistent with the reference path $\boldsymbol{Y}_{\text{ref}}$. An accuracy index function is designed based on the error between the two:

$$J_2\big(\boldsymbol{\Psi}(\Delta \boldsymbol{U})\big) = \big(\boldsymbol{Y}_{\text{ref}} - \boldsymbol{\Psi}(\Delta \boldsymbol{U})\big)^T \boldsymbol{Q}\big(\boldsymbol{Y}_{\text{ref}} - \boldsymbol{\Psi}(\Delta \boldsymbol{U})\big). \tag{15}$$

In the formula: $\boldsymbol{Q}$ is the weighting matrix.

For the control sequence $\boldsymbol{U}(\Delta \boldsymbol{U})$, based on the principle of comfort, it is desired that the control quantity maintains a relatively stable state. A comfort index function is designed based on the fluctuation of the control quantity:

$$J_3\big(\boldsymbol{U}(\Delta \boldsymbol{U})\big) = \beta_1 \sum_{i=0}^{N} |v_i - v_{\text{des}}| + \beta_2 \sum_{i=1}^{N-1} |v_i - v_{i-1}| + \beta_3 \sum_{i=1}^{N-1} |\delta_i - \delta_{i-1}|. \tag{16}$$

In the formula: $v_{\text{des}}$ represents the set reference vehicle speed; $v_i$ and $\delta_i$ represent the speed control quantity and front wheel steering angle control quantity at time $i$, respectively; $\beta_1$, $\beta_2$ and $\beta_3$ represent the weight coefficients, and satisfy $\beta_1 + \beta_2 + \beta_3 = 1$. The first term in $J_3$ represents the consistency of control vehicle speed with reference vehicle speed, the second term represents the fluctuation of control vehicle speed, and the third term represents the fluctuation of control steering.

In summary, the integrated planning and control objective function is defined as:

$$J(\Delta \boldsymbol{U}) = k_1 J_1\big(\boldsymbol{\Psi}(\Delta \boldsymbol{U})\big) + k_2 J_2\big(\boldsymbol{\Psi}(\Delta \boldsymbol{U})\big) + k_3 J_3\big(\boldsymbol{U}(\Delta \boldsymbol{U})\big). \tag{17}$$

In the formula: $k_1$, $k_2$, $k_3$ are the weights for safety, accuracy, and comfort, respectively, and satisfying $k_1 + k_2 + k_3 = 1$.

### 3.5. Optimization problem of integrated planning and control

The autonomous driving integrated planning and control problem is described as: solving for the optimal decision variable $\Delta \boldsymbol{U}$ to minimize the objective function $J$ while satisfying the system's constraint conditions.

Due to the characteristic limitations of the vehicle's actuator, the control quantity can only vary within an allowable range. For the front wheel steering angle

control quantity $\delta$, due to the mechanical structure limitations of the steering system, a limit constraint is needed: $|\delta| \leqslant \delta_{\max}$, and for the comfort of passengers, a limit constraint on the rate of change is also needed: $|\delta'| \leqslant \delta'_{\max}$, where $\delta_{\max}$ and $\delta'_{\max}$ represent the maximum front wheel steering angle and angular velocity, respectively; for the vehicle speed control quantity $v$, it needs to be limited within a safe vehicle speed: $|v| \leqslant v_{\max}$; its acceleration is also controlled within a reasonable range: $|v'| \leqslant v'_{\max}$, where $v_{\max}$ and $v'_{\max}$ represent the maximum control vehicle speed and acceleration, respectively. Define $\boldsymbol{u}_{\max} = [\delta_{\max}, v_{\max}]^T$, $\Delta\boldsymbol{u}_{\max} = [\delta'_{\max}, v'_{\max}]^T$, and let $G(\Delta\boldsymbol{U}) = [|\boldsymbol{U}(\Delta\boldsymbol{U})|, |\Delta\boldsymbol{U}|]^T$, the constraint conditions are designed as:

$$G(\Delta\boldsymbol{U}) = \begin{bmatrix}\boldsymbol{U}(\Delta\boldsymbol{U}) & \Delta\boldsymbol{U}\end{bmatrix}^T \leqslant \boldsymbol{U}_{\max}\,. \tag{18}$$

In the formula: $\boldsymbol{U}_{\max} = [\boldsymbol{u}_{\max}, \boldsymbol{u}_{\max}, \ldots, \boldsymbol{u}_{\max}, \Delta\boldsymbol{u}_{\max}, \Delta\boldsymbol{u}_{\max}, \ldots, \Delta\boldsymbol{u}_{\max}]^T$.

In summary, the mathematical model of the autonomous driving integrated planning and control optimization problem is:

$$\begin{cases}\min J(\Delta\boldsymbol{U}) \\ \text{s.t.}\;\; G(\Delta\boldsymbol{U}) \leqslant \boldsymbol{U}_{\max}\,.\end{cases} \tag{19}$$

## 4. User's steering style identification

Steering amplitude and steering speed are the main elements of user's driving style. User exhibits different steering amplitudes and speeds under various vehicle speed conditions, and different users show personalized differences in their steering styles. To identify user's personalized steering style, natural driving data is collected, and personalized steering style curves are generated using the method of least squares fitting.

### 4.1. Natural driving data collection

A natural driving data collector was designed with the STM32 microcontroller as the main control chip. The collector integrates two serial communication interfaces, connected respectively to the positioning module and the steering encoder, to collect the vehicle's real-time speed and steering angle. The collector is deployed on a Buick Verano 1.5T experimental vehicle, as shown in Figure 5. In manual driving mode, the collector samples at a 100ms interval, obtaining natural driving data from the user, including vehicle speed, steering angle, and steering angular velocity.

The vehicle speed $v$, steering angle $\delta$, and steering angular velocity $\omega$ form a set of natural driving data (data $= [v, \delta, \omega]$). Each set of valid natural driving data

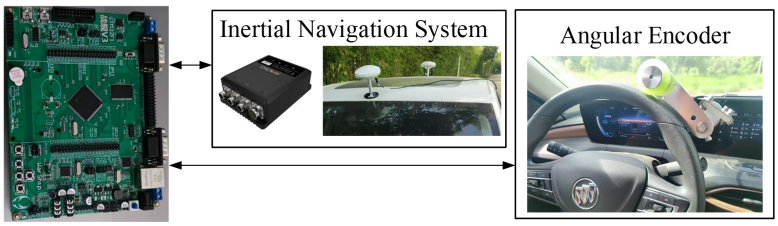


Figure 5: Deployment of driving data acquisition system

is processed to retain the maximum steering angle and angular velocity at various speed values, serving as driving style sample data. After a period of manual driving, a collection of user's style sample data $D^* = \{D_1^*, D_2^*, D_3^*, \ldots, D_n^*, \ldots, D_N^*\}$ is obtained. Here, $D_n^* = [V_n^*, \delta_n^*, \omega_n^*]$, where $V_n^*$ is the discrete speed value, $\delta_n^*$ is the maximum steering angle within the speed range $[V_n^* - V_0, V_n^* + V_0]$, and $\omega_n^*$ is the maximum steering angular velocity within the same speed range. As shown in Figure 6, the natural driving data obtained by the user over a period of driving, as well as the processed user's style sample data.

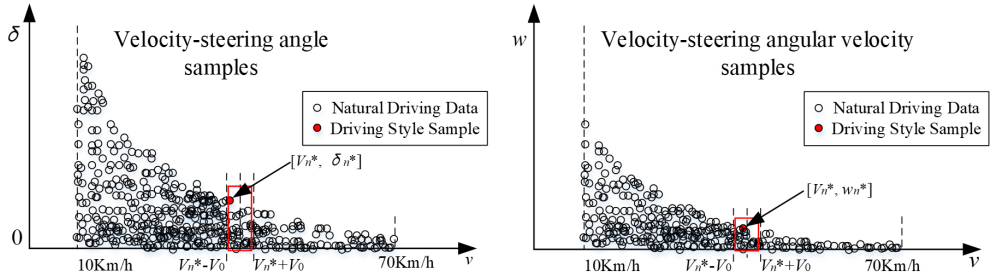


Figure 6: User's natural driving data and style sample data

### 4.2. Steering style curve identification

Based on the collected user's driving style sample data set, the user's steering style curves, including the speed-steering angle curve and the speed-steering angular velocity curve, are identified using the method of least squares. Considering the characteristics of user's steering styles, hyperbolic functions are used to fit the driving style curves, that is:

$$c_1 = a_1 \frac{1}{v} + a_2 \,, \tag{20}$$

$$c_2 = b_1 \frac{1}{v} + b_2 \,. \tag{21}$$

In the formulas: $v$ represents the vehicle's speed, $c_1$ represents the maximum steering angle at speed $v$, $c_2$ represents the maximum steering angular velocity at speed $v$, $a_1$ and $a_2$ are the speed-steering curve coefficients, and $b_1$ and $b_2$ are the speed-steering angular velocity curve coefficients.

Based on the driving style sample data set $D^*$, construct the speed-steering curve sample set $A$ and the speed-steering angular velocity curve sample set $B$, respectively:

$$A = \left\{ \left[V_1^*, \delta_1^*\right], \left[V_2^*, \delta_2^*\right], \cdots, \left[V_N^*, \delta_N^*\right] \right\}, \tag{22}$$

$$B = \left\{ \left[V_1^*, \omega_1^*\right], \left[V_2^*, \omega_2^*\right], \cdots, \left[V_N^*, \omega_N^*\right] \right\}. \tag{23}$$

The method of least squares cannot directly fit hyperbolic function curves, requiring necessary transformations. Taking the speed-steering curve as an example, let $X = 1/v$ and $Y = c_1$, construct a linear polynomial function: $Y = a_1 X + a_2$, and the sample set:

$$A^* = \left\{ \left[\frac{1}{V_1^*}, \delta_1^*\right], \left[\frac{1}{V_2^*}, \delta_2^*\right], \cdots, \left[\frac{1}{V_N^*}, \delta_N^*\right] \right\}. \tag{24}$$

Given the sample set $[X, Y]$ and the fitting equation $Y = a_1 X + a_2$, according to the principle of least squares, solve for the optimal fitting coefficients $a_1^*$ and $a_2^*$ to obtain the speed-steering fitting curve:

$$c_1 = a_1^* \frac{1}{v} + a_2^*. \tag{25}$$

Similarly, obtain the speed-steering angular velocity fitting curve:

$$c_2 = b_1^* \frac{1}{v} + b_2^*. \tag{26}$$

### 4.3. Experimental study

Three users with different driving styles were selected to drive the experimental vehicle for 100 kilometers. Based on the user's natural driving data and the user style curve identification method, a user driving style identification experiment was conducted. The experimental results are shown in Figure 7, where the three users are defined as Style 1 (Driver 1), Style 2 (Driver 2), and Style 3 (Driver 3).

From the experimental results, it can be seen that the common feature of the steering style curves of the three users is that the steering angular velocity decreases as the vehicle speed increases. This feature reflects the requirements of safe driving, i.e., avoiding sudden changes in steering at high speeds to cause

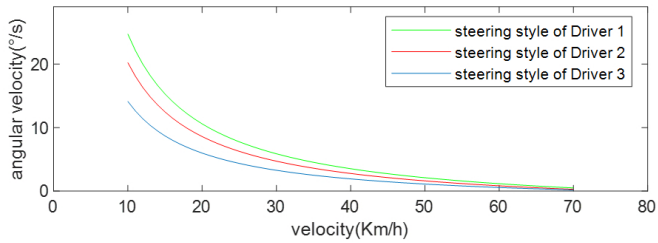


Figure 7: Driving style curves of different users

rollover. Different users show personalized different characteristics: under different vehicle speed conditions, the amplitude of the steering angular velocity is different. For example, Style Curve 1 has a larger steering angular velocity at every speed state, hence a more aggressive steering style; Style Curve 3 has a smaller steering angular velocity, hence a more conservative steering style; and Style Curve 2 is moderate.

## 5. Optimization solution considering steering style

For the integrated planning and control optimization problem and the identified user's steering style curves, a genetic algorithm that considers steering style is used to find the optimal steering control quantity. The overall idea is to: represent the decision variables as an individual, construct an initial population; based on user's steering style factors, perform decoding operations on population individuals; use the objective function as the evaluation criterion, and according to the rules of genetic evolution, transform the initial population to gradually enhance the comprehensive performance of population individuals until optimal; finally, decode the optimal individual into the optimal control quantity to implement the steering control of intelligent vehicles.

### 5.1. Population initialization

The decision variable is designed as a control increment sequence for the future time domain: $\Delta \boldsymbol{U} = [\Delta \boldsymbol{u}_0, \Delta \boldsymbol{u}_1, \Delta \boldsymbol{u}_2, \ldots, \Delta \boldsymbol{u}_n, \ldots, \Delta \boldsymbol{u}_{N-1}]$, and the decision variable is treated as an individual in the population, represented by a binary string:

$$\begin{cases} P = V_0 V_1 V_2 \cdots V_n \cdots V_{N-1}\,, \\ V_i = A_1 A_2 A_3 \cdots A_i \cdots A_I\,, \\ A_i = 0 \ \text{ or } \ 1. \end{cases} \tag{27}$$

In the formula: $I$ represents the number of bits in each binary substring, so the total number of bits in the individual binary string is $N \times I$.

The $n$-th substring sequence $V_n$ in the individual binary string represents the $n$-th decision quantity in the control increment sequence. For an autonomous driving vehicle, $V_n$ represents the control increment $\Delta \boldsymbol{u}_n$ at time $n$ in the future, where the first $I/2$ bits of the binary string represent the steering control increment $\Delta\delta_n$, and the last $I/2$ bits represent the speed control increment $\Delta v_n$. Following the basic principles of genetic algorithms, a population consisting of $P$ individuals is constructed, and the binary strings are randomly assigned initial values of 0 or 1, as shown in Figure 8.

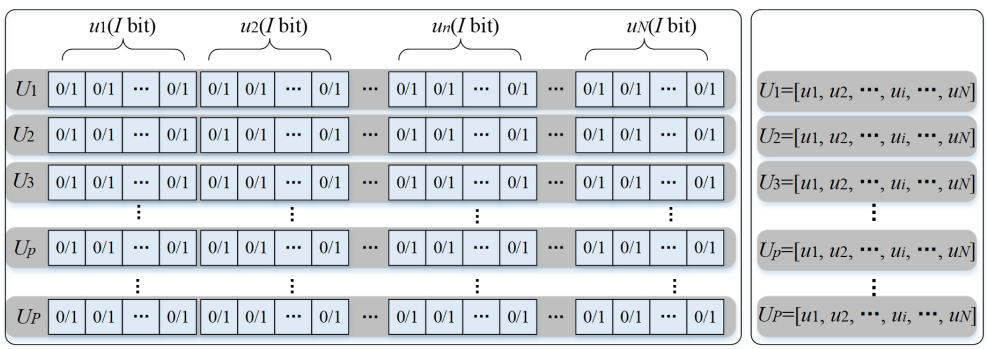


Figure 8: Encoding form of individuals

### 5.2. Decoding method based on steering style factors

The steering style curve describes the user's steering habits under different vehicle speed conditions. Assuming the vehicle speed at a certain moment is $v_c$, and the vehicle speed will not change drastically in a short period, the maximum steering angle and maximum steering angular velocity of the user during this period can be solved according to the steering style curve, respectively defined as the steering angle style factor $C_1$ and the steering angular velocity style factor $C_2$:

$$C_1 = \left(a_1 \frac{1}{v_c} + a_2\right) / iw_0 \,, \tag{28}$$

$$C_2 = \left(b_1 \frac{1}{v_c} + b_2\right) / iw_0 \,. \tag{29}$$

In the formulas: $iw_0$ is the steering transmission ratio.

Based on the steering style factors, the individual chromosome is decoded. For the $n$-th decision variable binary substring $V_n$, its corresponding steering

angle is decoded as:

$$\Delta u_i = C_2 \left( \frac{2b_m}{2^{I/2} - 1} - 1 \right). \tag{30}$$

In the formula: $b_m$ represents the decimal number corresponding to the first $I/2$ bits of the $I$-bit binary substring $V_n$.

Assuming the steering control quantity of the last control cycle is $\delta_{\text{pre}}$, then the steering control quantity at time $n$ is: $\delta_n = \delta_{\text{pre}} + \Delta\delta_0 + \Delta\delta_1 + \Delta\delta_2 + \ldots + \Delta\delta_n$. When $\delta_n > C_1$, take $\delta_n = C_1$; when $\delta_n < -C_1$, take $\delta_n = -C_1$.

The decoding method, which considers the steering style factors, ensures that the change increment of the steering angle does not exceed the steering angular velocity factor, and the steering angle does not exceed the steering angle factor, thus decoding the control sequence that satisfies the user's steering style constraints.

### 5.3. Vehicle motion path prediction

For each individual after decoding, a corresponding control sequence can be generated. Let the control sequence corresponding to the $p$-th individual be:

$$\boldsymbol{U}(p) = \left\{ [\delta_0, v_0],\ [\delta_1, v_1],\ [\delta_2, v_2],\ \ldots,\ [\delta_N, v_N] \right\}. \tag{31}$$

Considering the simplification of the problem, it is assumed that the vehicle speed is constant within the prediction time domain. To verify the feasibility of the method, this paper uses a vehicle kinematics model to describe the vehicle's motion characteristics [17, 18]:

$$\begin{cases} x' = v\cos\theta, \\ y' = v\sin\theta, \\ \theta' = v\tan(\delta)/L. \end{cases} \tag{32}$$

In the formula: $[x, y, \theta]^T$ constitutes the state quantity $\boldsymbol{X}$; $[\delta, v]^T$ constitutes the control quantity $\boldsymbol{u}$.

Based on the vehicle kinematics model of equation (32), combined with the derivation process of equations (10)–(13), the vehicle travel route $\boldsymbol{\Psi}_p$ represented by the $p$-th individual can be predicted. By this method, the predicted trajectories $\boldsymbol{\Psi}_1, \boldsymbol{\Psi}_2, \boldsymbol{\Psi}_3, \ldots, \boldsymbol{\Psi}_P$ corresponding to all individuals in the current population can be obtained.

### 5.4. Genetic algorithm optimization solution

Genetic algorithms are methods that simulate the natural evolution process to search for optimal solutions, mainly including population initialization, encoding

and decoding, fitness calculation, selection replication, crossover mutation, and iterative evolution processes [19, 20]. Based on the general process of genetic algorithms, the optimization solution process for the integrated planning control problem considering steering style is designed as shown in Figure 9.

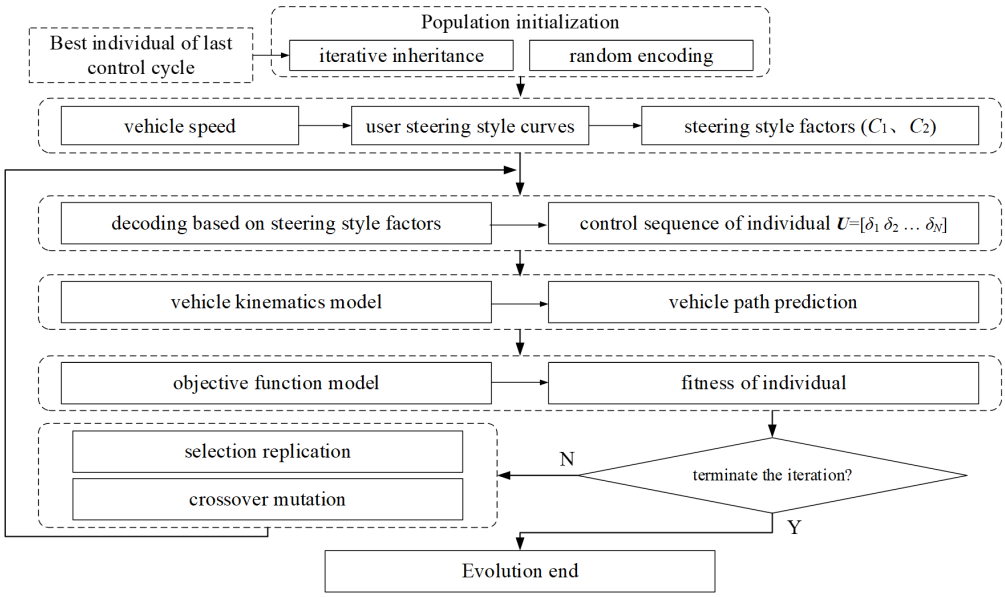


Figure 9: Optimal steering control quantity solving process

In the population initialization phase, by the principle of iterative inheritance, the optimal control increment sequence from the last control cycle is iterated into the current population, using a shift encoding method to generate a certain number of individuals, with the aim of retaining the excellent individuals from the last control cycle. Then, the remaining individuals of the initial population are encoded using a random encoding method, together forming a population of $P$ individuals for the control increment sequence of the next $N$ moments.

In the individual decoding phase, first, according to the current vehicle speed and user steering style curve, the steering style factors $C_1$ and $C_2$ are calculated. Then, based on the decoding method of steering style factors, each individual in the population is decoded into the corresponding future control sequence $\boldsymbol{U} = [\boldsymbol{u}_0, \boldsymbol{u}_1, \boldsymbol{u}_2, \ldots, \boldsymbol{u}_n, \ldots, \boldsymbol{u}_{N-1}]$.

In the individual fitness calculation phase, first, combine the vehicle kinematics model to predict the vehicle travel path $\boldsymbol{\Psi}$ represented by each individual. Then, according to the objective function model in Section 2, calculate the objective function value $J(\boldsymbol{U}, \boldsymbol{\Psi})$ of the control sequence represented by each individual.

According to the principle that the smaller the objective function value, the higher the individual fitness, the fitness function of the individual and the total fitness of the population are defined as: $\text{fitness}(i) = 1/J(i)$, $\text{fitness}_{\text{all}} = \sum \text{fitness}(i)$.

Set the maximum number of iterations $K$ and the minimum cost function value $J_{\min}$. Determine whether the current conditions meet the end of the iterative evolution, i.e., the current number of iterations exceeds $K$, or the cost function value of the optimal individual is less than $J_{\min}$. If satisfied, the evolution ends. If not satisfied, enter the selection replication and crossover mutation phase, using the classic roulette method to select individuals with better performance from the current population, define the probability of individual selection as formula (33), and produce the next generation of the population through crossover mutation.

$$p(i) = \frac{\text{fitness}(i)}{\text{fitness}_{\text{all}}}. \tag{33}$$

When the evolution process is completed, obtain the optimal individual $\Delta \boldsymbol{U}$, and through the decoding method based on the steering style factors, obtain the control sequence $\boldsymbol{u}_0^*, \boldsymbol{u}_1^*, \boldsymbol{u}_2^*, \ldots, \boldsymbol{u}_{N-1}^*$ corresponding to the optimal individual, and take the first control quantity $\boldsymbol{u}_0^*(\delta_0^*)$ as the output of the current control cycle, sending it to the actuator to implement the vehicle's steering control.

## 6. Simulation experimental study

This section verifies the proposed method through simulation experiments. First, a planning and control system simulation model is designed to validate the feasibility of the integrated planning and control strategy in typical driving scenarios. Then, the factor of user's driving style is introduced to demonstrate the good performance of the planning and control method that considers user's driving style. Finally, the impact of different users' driving styles on autonomous driving planning and control is studied through simulation.

### 6.1. Simulation of integrated planning and control

#### 6.1.1. Simulation model

A simulation model is established in the MATLAB environment, as shown in Figure 10. The path generator outputs a reference path ref_path that includes planar coordinate information based on the vehicle's position; the obstacle module is used to manually/randomly set the position coordinates of obstacles on the road; the speed module is used to set the target vehicle speed. The integrated planning controller, based on the input information, uses a genetic algorithm to solve for the optimal control quantity $\delta^*$ (assuming constant vehicle speed during driving for simplified design); the vehicle motion calculation module calculates the motion

increment for the next control cycle based on the control quantity input $(\delta^*,\ v)$ using a vehicle kinematics model and outputs the real-time pose information $(x, y, \theta)$ of the vehicle combined with a position solver.

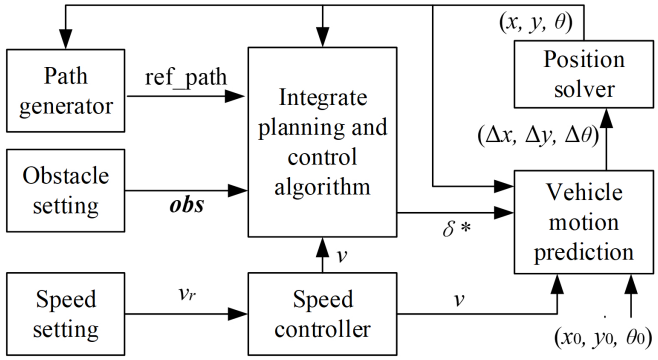


Figure 10: Integrated planning and control simulation model

The integrated planning and control method based on the genetic algorithm is used, with the population size $P$ set to 30; the prediction time domain is set to 5 seconds, the control cycle $T$ is set to 0.1 seconds, and the encoding length is 8 bits (front wheel steering angle increment encoding); the control increment limit is related to real-time vehicle speed; the maximum number of iterations is set to 100.

#### 6.1.2. Static obstacle scenario simulation

The performance of the intelligent vehicle driving on straight and curved roads is simulated, with the reference path set to a total length of 300 meters, creating a 3-lane driving scenario with an additional lane on either side of the reference path, each lane being 3.5 meters wide; static obstacle coordinates along the reference path are set to $(50, 0.5)$, $(150, -0.5)$, and $(250, 1.0)$; the vehicle's initial pose is set to $[x_0, y_0, \theta_0]^T = [0, 0, 0]^T$; the target vehicle speed is set to 40 Km/h; the vehicle wheelbase is set to $L = 2.5$ m. Simulation results are shown in Figures 11–14.

According to the simulation results, before encountering static obstacles, the vehicle changes its driving route in advance through steering control, maintaining a safe distance from the obstacles and passing safely. It has good safety performance and can quickly track back to the reference path after obstacle avoidance. In sections without static obstacles, the vehicle's lateral deviation is small, indicating high tracking accuracy. Throughout the driving process, the fluctuation range of the vehicle's front wheel steering angle control quantity is small, ensur-

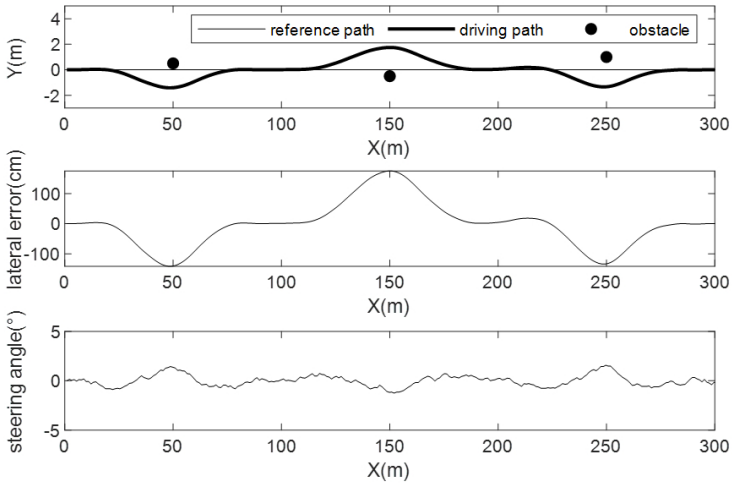


Figure 11: Simulation results of straight road scenario

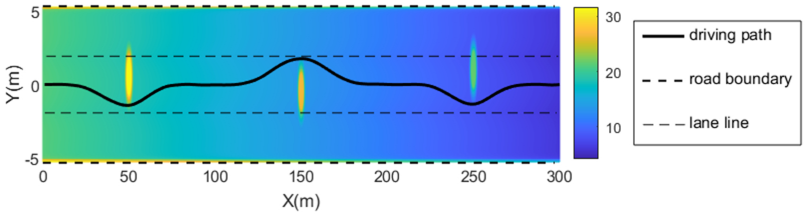


Figure 12: Global potential field map of straight road

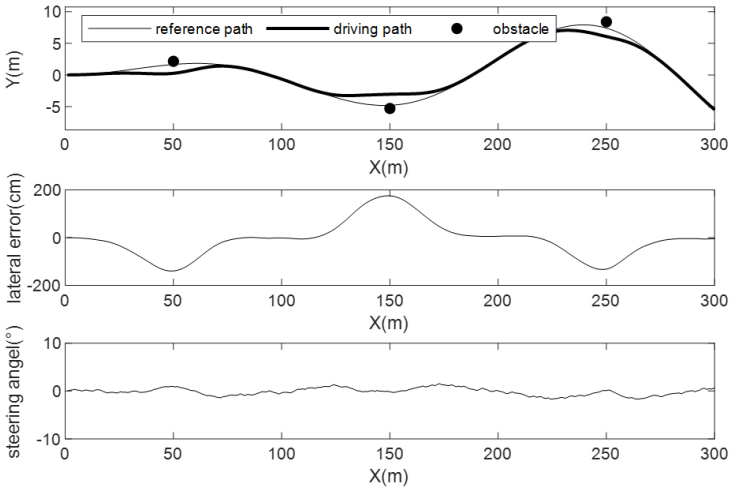


Figure 13: Simulation results of curved road scenario

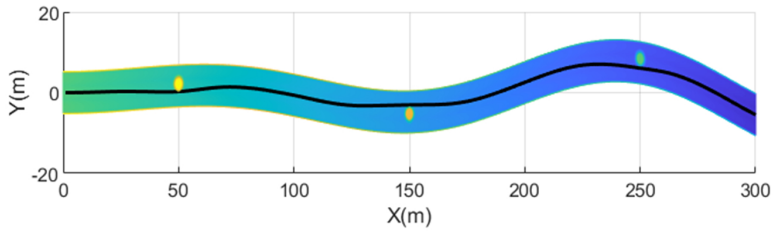


Figure 14: Global potential field map of curved road

ing good driving comfort. From the global view, the intelligent vehicle's driving path is always in the direction of the minimum potential field value.

#### 6.1.3. Dynamic obstacle scenario simulation experiment

The driving performance of the intelligent vehicle when encountering dynamic obstacles is simulated, with the reference path set to a total length of 300 meters, creating a 3-lane driving scenario with an additional lane on either side of the reference path, each lane being 3.5 meters wide; dynamic obstacles are set along the reference path; the vehicle's initial pose is set to $[x_0, y_0, \theta_0]^T = [0, 0, 0]^T$; the target vehicle speed is set to 40 Km/h; the vehicle wheelbase is set to $L = 2.5$ m. Simulation results are shown in Figures 15–18.

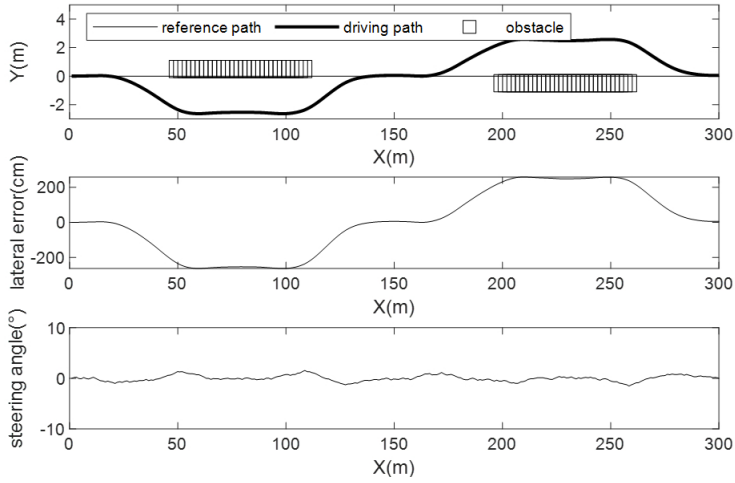


Figure 15: Simulation results of straight road scenario

The above experiments show that before encountering dynamic obstacles, the vehicle changes its driving route in advance through steering control, maintaining a safe distance from the obstacles and continuously completing overtaking of low-

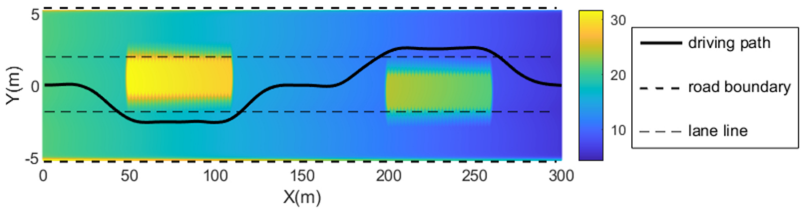


Figure 16: Global potential field map of straight road

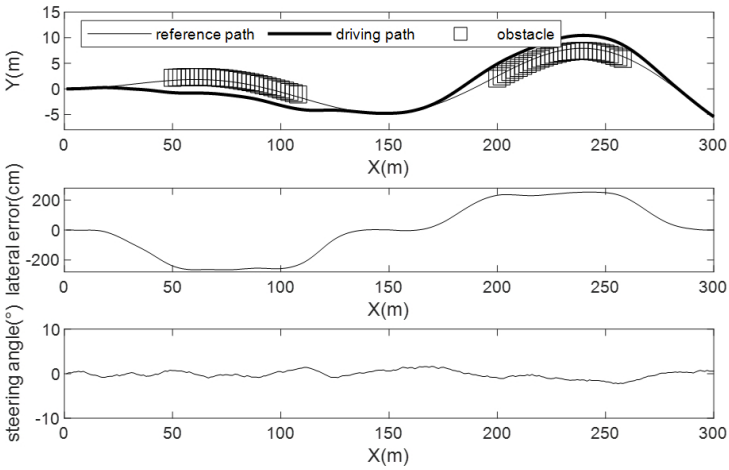


Figure 17: Simulation results of curved road scenario

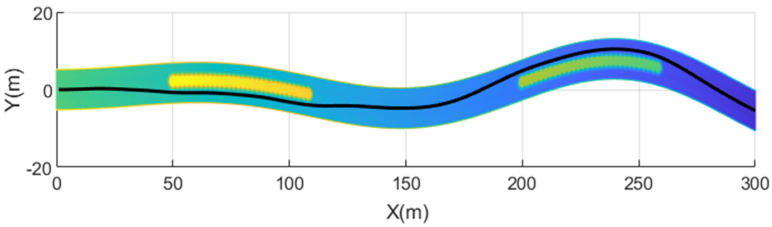


Figure 18: Global potential field map of curved road

speed dynamic obstacles. After overtaking, the intelligent vehicle resumes driving on the reference path. In sections without obstacles, the vehicle's lateral deviation is small, indicating high tracking accuracy. Throughout the driving process, the fluctuation range of the vehicle's front wheel steering angle control quantity is small, ensuring good driving comfort. From the global view, the intelligent vehicle's driving path is always in the direction of the minimum potential field value.

### 6.2. Simulation experiment considering user's steering style

#### 6.2.1. Simulation model

A simulation model is established in the MATLAB environment, as shown in Figure 19. The path generator outputs a reference path ref_path that includes planar coordinate information based on the vehicle's position; the obstacle module is used to manually/randomly set the position coordinates of obstacles on the road; the speed module is used to set the target vehicle speed. The integrated planning controller, based on the input information, uses a genetic algorithm to solve for the optimal control quantity $\delta^*$ (assuming constant vehicle speed during driving for simplified design); the vehicle motion calculation module calculates the motion increment for the next control cycle based on the control quantity input $(\delta^*,\ v)$ using a vehicle kinematics model and outputs the real-time pose information $(x, y, \theta)$ of the vehicle combined with a position solver.

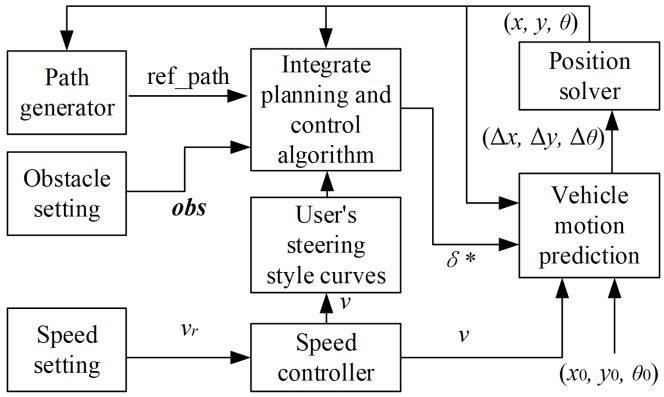


Figure 19: Simulation model of integrated planning and control considering user's steering style

#### 6.2.2. Experiment of planning and control system considering user's steering style

The experimental results of Driver 2 are selected for simulation research, and the steering angular velocity style curve is shown in Figure 20. Based on Driver 2's steering angular velocity style curve, the steering style factors are calculated to simulate the driving characteristics of an autonomous vehicle in a straight road obstacle avoidance scenario. The reference path is set to a total length of 300 meters, the vehicle's initial pose is set to $[x_0, y_0, \theta_0]^T = [0, 0, 0]^T$; obstacle positions are set to $[100, 0.5]$ and $[250, -0.5]$; vehicle speeds are set to 20 Km/h, 40 Km/h, and 60 Km/h, respectively. Simulation results are shown in Figure 21.

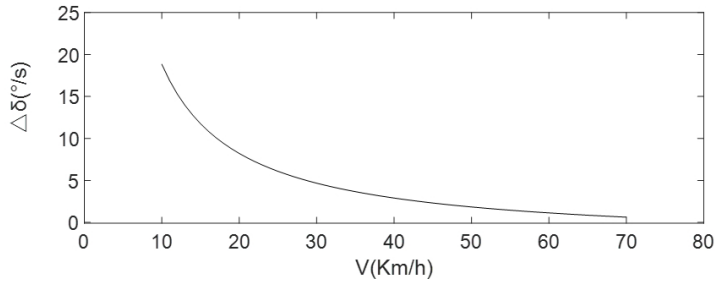


Figure 20: Velocity-steering angular velocity style curve

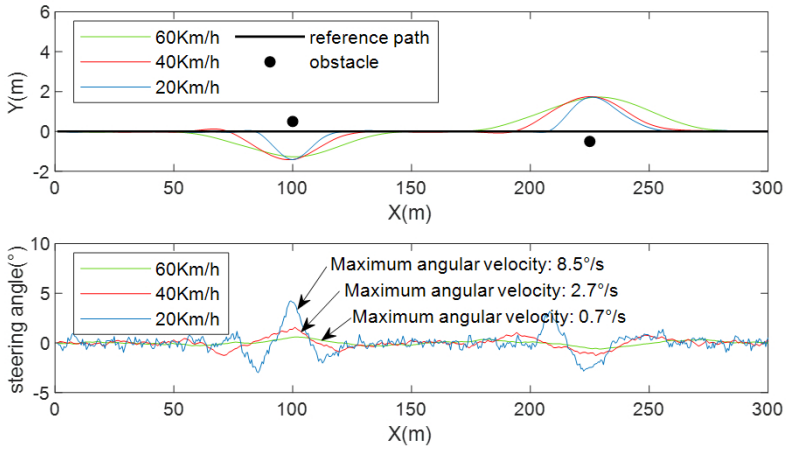


Figure 21: Simulation results considering user's steering style

According to the simulation results, under the three vehicle speed conditions, the steering style factors for the user are different, resulting in different steering control quantities and driving paths. When driving at a speed of 60 Km/h, the steering style factor is smaller, hence the decoded control increment sequence and control quantity sequence are smaller, with the smallest amplitude and rate of change of the front wheel steering angle, and the autonomous vehicle starts to change lanes to avoid obstacles at a point farther from the obstacles. When driving at a speed of 20 Km/h, the steering style factor is larger, hence the decoded control increment sequence and control quantity sequence are larger, with the largest amplitude and rate of change of the front wheel steering angle, and the autonomous vehicle starts to change lanes to avoid obstacles at a point closer to the obstacles. The results show that the lateral control strategy based on user steering style adapts to the common characteristics of users, i.e., the steering angular velocity decreases as the vehicle speed increases.

#### 6.2.3. Comparative simulation experiment

The experimental results of Driver 2 were selected for comparative simulation studies to examine the differences between considering user steering style and not considering user's steering style. When not considering user's steering style, the maximum steering angular velocity was set to a fixed 3°/s. The driving characteristics of an autonomous vehicle in a straight road obstacle avoidance scenario were simulated. The reference path was set to a total length of 450 meters, with the vehicle's initial pose as $[x_0, y_0, \theta_0]^T = [0, 0, 0]^T$; obstacle positions were set to [50, 0.5], [130, 0.5], and [400, 0.5]; the simulated vehicle speed accelerated from 0 to 60 Km/h. The simulation results are shown in Figure 22.

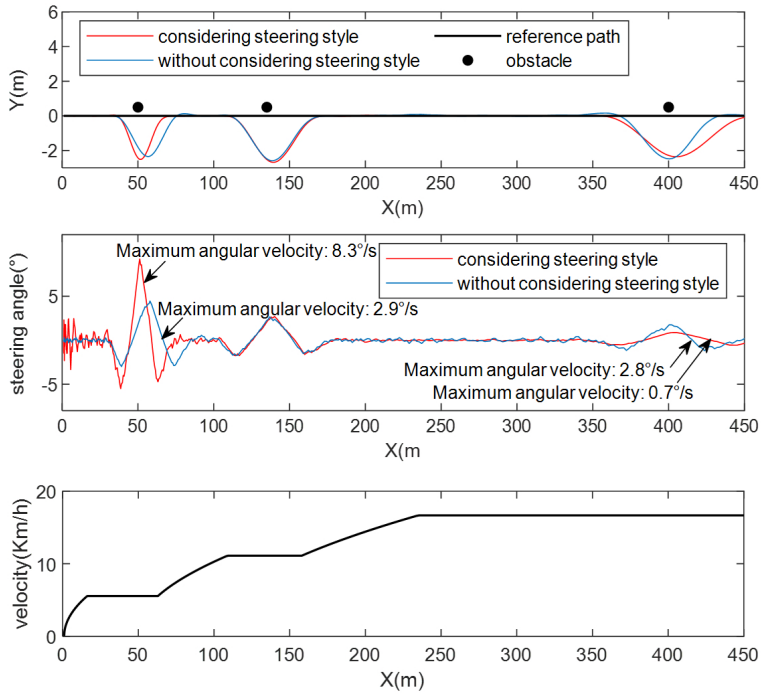


Figure 22: Simulation results with considering user's style and without considering user's style

According to the simulation results, when not considering user's steering style, the front wheel steering angle control quantity struggled to adapt to full-speed autonomous driving. At low speeds (20 Km/h), the front wheel steering angle change rate considering user's steering style was larger, capable of adapting to quick lane changes for obstacle avoidance, whereas the front wheel steering angle change rate without considering user's steering style was insufficient, leading to a slow obstacle avoidance process that did not match the user's steering style. At medium speeds (40 Km/h), the front wheel steering angle change rates with and

without considering user's steering style were close, and both had consistent lane change and obstacle avoidance processes. At high speeds (60 Km/h), the front wheel steering angle change rate considering user's steering style was smaller, avoiding the risk of rolling over, while the front wheel steering angle change rate without considering user steering style was excessive, leading to an aggressive lane change and obstacle avoidance process with a risk of rolling over, thus not matching the user's steering style.

### 6.3. Comparative experiment of different users' styles

The steering styles of three drivers were applied to the autonomous driving planning and control strategy to simulate the driving characteristics of an autonomous vehicle in a straight road obstacle avoidance scenario. The reference path was set to a total length of 500 meters, with the vehicle's initial pose as $[x_0, y_0, \theta_0]^T = [0, 0, 0]^T$; obstacle positions were set to [50, 0.5], [130, 0.5], and [400, 0.5]; the simulated vehicle speed accelerated from 0 to 60 Km/h. The simulation results are shown in Figure 23.

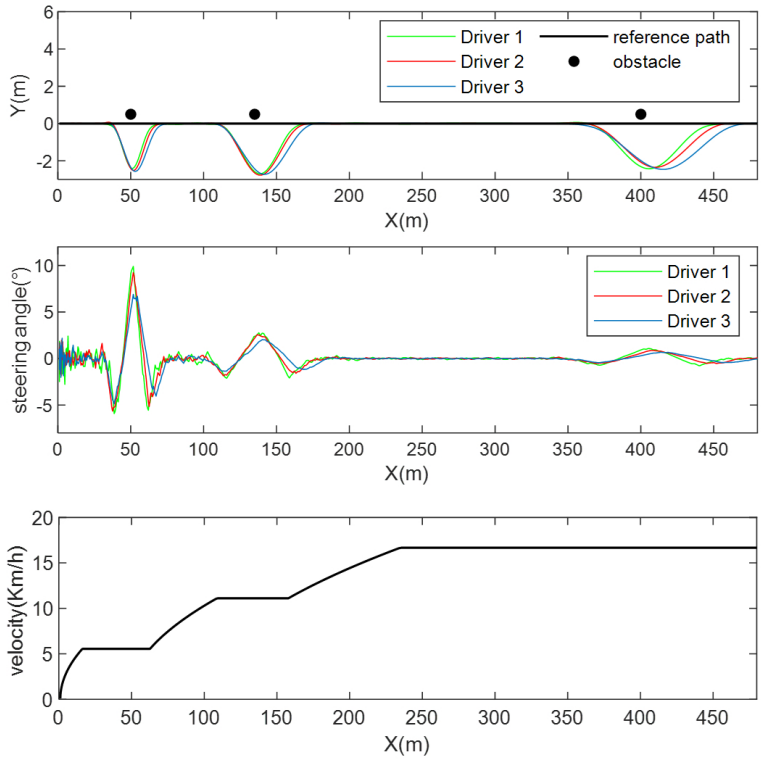


Figure 23: Comparison experiment considering different users' styles

The simulation results indicate that under the same vehicle speed conditions, the autonomous driving lateral control algorithms with three different steering styles output different steering control quantities, resulting in different driving paths for the vehicle. Style 1, which tends to be aggressive, has the largest amplitude and rate of change in steering control, thus exhibiting a "quick lane change, quick return to center" phenomenon during obstacle avoidance; Style 3, which tends to be conservative, has a more gradual amplitude and rate of change in steering control, resulting in a "slow lane change, slow return to center" phenomenon during obstacle avoidance. The simulation results validate that the lateral control strategy considering user's steering style adapts to the personalized differences of users, that is, the steering speed styles of different users, thereby resolving steering style conflicts.

## 7. Conclusions

This paper utilizes natural driving data from user for the identification of steering styles and applies it to personalized steering control of autonomous vehicle. By employing artificial potential field theory and optimal control theory, an integrated planning and control optimization problem mathematical model was constructed. A user natural driving data collection system was designed to achieve the identification of user's steering style curves. Algorithm based on user's steering style factors was proposed for decoding, and a genetic algorithm was used to find the optimal steering control quantity, thereby achieving personalized planning and control of autonomous vehicles. An integrated planning and control simulation model for autonomous driving that considers user's steering style was built, validating the feasibility of the proposed integrated planning and control method in typical scenarios. It realized the adaptation of autonomous vehicle steering control style to user's driving style, providing an anthropomorphic strategy for autonomous driving planning and control.

## References

[1] P. Wang, H. Li and C.Y. Chan: Meta-adversarial inverse reinforcement learning for decision-making tasks. *2021 IEEE International Conference on Robotics and Automation (ICRA)*, (2021), DOI: 10.48550/arXiv.2103.12694

[2] H. Li, C. Wu, D. Chu, L. Lu and K. Cheng: Combined trajectory planning and tracking for autonomous vehicle considering driving styles. *IEEE Access*, **99**, (2021), 9453–9463, DOI: 10.1109/ACCESS.2021.3050005

[3] F. Hartvich, M. Beggiato and J.F. Krems: Driving comfort, enjoyment and acceptance of automated driving effects of drivers' age and driving style familiarity. *Ergonomics*, **61**(8), (2018), 1017–1032, DOI: 10.1080/00140139.2018.1441448

[4] N.M. Yusof, J. Karjanto, J. Terken, F. Delbressine, M.Z. Hassan and M. Rauterberg: The exploration of autonomous vehicle driving styles: Preferred longitudinal, lateral, and vertical accelerations. *Proceedings of the 8th International Conference on Automotive User Interfaces and Interactive Vehicular Applications*, (2016), DOI: 10.1145/3003715.3005455

[5] P. Lin, J.H. Yang, Y.S. Quan and C.C. Chung: Potential field-based path planning for emergency collision avoidance with a clothoid curve in waypoint tracking. *Asian Journal of Control*, **24**(3), (2022), 1074–1087, DOI: 10.1002/asjc.2778

[6] C. Gkartzonikas and K. Gkritza: What have we learned? A review of stated preference and choice studies on autonomous vehicles. *Transportation Research Part C: Emerging Technologies*, **98**, (2019), 323–337, DOI: 10.1016/j.trc.2018.12.003

[7] C. Zhang, D. Chu, S. Liu, Z. Deng, C. Wu and X. Su: Trajectory planning and tracking for autonomous vehicle based on state lattice and model predictive control. *IEEE Intelligent Transportation Systems Magazine*, **11**(2), (2019), 29–40, DOI: 10.1109/MITS.2019.2903536

[8] A. Tampuu, M. Semikin, N. Muhammad, D. Fishman and T. Matiisen: A survey of end-to-end driving: Architectures and training methods. *IEEE Transactions on Neural Networks and Learning Systems*, **99**, (2020), 1–21, DOI: 10.1109/TNNLS.2020.3043505

[9] C. Daniel and M. Oliveira: A review of end-to-end autonomous driving in urban environments. *IEEE Access*, **10**, (2022), 75296–75311, DOI: 10.1109/ACCESS.2022.3192019

[10] L. Chen, P. Wu, K. Chitta, B. Jaeger and A. Geiger: End-to-End Autonomous Driving: Challenges and Frontiers. *IEEE Transactions on Pattern Analysis and Machine Intelligence*, **46**(12), (2024), 10164–10183, DOI: 10.1109/TPAMI.2024.3435937

[11] B. Sun, W. Deng, J. Wu, Y. Li and J. Wang: An intention-aware and online driving style estimation based personalized autonomous driving strategy. *International Journal of Automotive Technology*, **21**(6), (2020), 1431–1446, DOI: 10.1007/s12239-020-0135-3

[12] B. Peng, Q. Sun, S.E. Li, D. Kum and T. Gu: End-to-end autonomous driving through dueling double deep Q-network. *Automotive Innovation*, **4**, (2021), 328–337, DOI: 10.1007/s42154-021-00151-3

[13] J. Liu, L.N. Boyle and A.G. Banerjee: An inverse reinforcement learning approach for customizing automated lane change systems. *IEEE Transactions on Vehicular Technology*, **71**(9), (2022), 9261–9271, DOI: 10.1109/TVT.2022.3179332

[14] P. Wang, S. Gao, L. Li, B. Sun and S. Cheng: Obstacle avoidance path planning design for autonomous driving vehicles based on an improved artificial potential field algorithm. *Energies*, **12**, (2019), 2342, DOI: 10.3390/en12122342

[15] V. Asodia, Z. Feng and S. Fallah: Human-aligned longitudinal control for occluded pedestrian crossing with visual attention. *2024 IEEE International Conference on Robotics and Automation (ICRA)*, (2024), DOI: 10.1109/ICRA57147.2024.10611046

[16] A. Sallab, M. Abdou, E. Perot and S. Yogamani: Deep reinforcement learning framework for autonomous driving. *Electronic Imaging*, **19**, (2017), 70–76, DOI: 10.2352/ISSN.2470-1173.2017.19.AVM-023

[17] M. Wang, J. Chen, H. Yang, X. Wu and L. Ye: Path tracking method based on model predictive control and genetic algorithm for autonomous vehicle. *Mathematical Problems in Engineering*, **49**, (2022), 1–16, DOI: 10.1155/2022/4661401

[18] X. Zhijiang, Z. Wanzhong, W. Chunyan and D. Yifan: Local path planning and tracking control of vehicle collision avoidance system,. *Transaction of Nanjing University of Aeronautics and Astronautics*, **35**(4), (2018), 729–738, DOI: 10.16356/j.1005-1120.2018.04.729

[19] F. Schockenhoff, M. Zähringer, M. Brönner and M. Lienkamp: Combining a genetic algorithm and a fuzzy system to optimize user centricity in autonomous vehicle concept development. *Systems*, **9**(2), (2021), 25, DOI: 10.3390/systems9020025

[20] J. Chen and G. Tian: A tuning method for speed tracking controller parameters of autonomous vehicles. *Applied Sciences*, **14**(22), (2024), 10209, DOI: 10.3390/app142210209